Macromolecules

Article

pubs.acs.org/Macromolecules

Salt Dependence of the Chain Stiffness and Excluded-Volume Strength for the Polymethacrylate-Type Sulfopropylbetaine in Aqueous NaCl Solutions

Moriya Kikuchi,[†] Yuki Terayama,[‡] Tatsuya Ishikawa,[‡] Taiki Hoshino,[†] Motoyasu Kobayashi,[†] Noboru Ohta,[∥] Hiroshi Jinnai,[†] and Atsushi Takahara*[,†,‡,§]

[†]ERATO, Takahara Soft Interfaces Project, Japan Science and Technology Agency, 744 Motooka, Nishi-ku, Fukuoka 819-0395, Japan

[‡]Graduate School of Engineering and [§]Institute for Materials Chemistry and Engineering, Kyushu University, 744 Motooka, Nishi-ku, Fukuoka 819-0395, Japan

[∥]Japan Synchrotron Radiation Research Institute/Spring-8, 1-1-1, Kouto, Sayo-cho, Sayo-gun, Hyogo 679-5198, Japan

Supporting Information

ABSTRACT: A series of zwitterionic polyelectrolytes poly[3-(*N*-2-methacryloyloxyethyl-*N*,*N*-dimethyl)ammonatopropanesulfonate] (PMAPS) with a wide range of weight-average molecular weight (M_w) between 5.5×10^3 and 1.6×10^6 g mol^{-1} with narrow molecular weight distribution (M_w/M_n = 1.07−1.19) were thoroughly characterized in aqueous NaCl solutions for salt concentration (C_s) over a range from theta C_s (0.074 M) to 1.0 M by synchrotron radiation small-angle X-ray scattering (SAXS), light scattering, and viscometry at 25 °C. To determine the chain stiffness parameter (λ^{-1}) and the excluded-volume strength (B) of PMAPS in an aqueous NaCl solution, SAXS profiles and the M_w dependences of the radius of gyration, the second virial coefficient, the interpenetration function, the hydrodynamic radius, and the intrinsic viscosity for PMAPS were analyzed on the basis of the (un)perturbed cylindrical wormlike chain model. The experimental λ^{-1} value for PMAPS chains in aqueous NaCl solutions barely decreased but was almost constant with the increasing C_s, whereas the value of B was increased gradually with the increasing C_s. Thus, the dominant factor for the chain dimension of PMAPS in aqueous NaCl solutions was the long-range interaction (i.e., B) than the short-range interaction (i.e., λ^{-1}). The observed C_s dependences of λ^{-1} and B for PMAPS chains in aqueous NaCl solutions were fairly described by the theories of the polyampholyte with the nonrepulsive, the repulsive, and the attractive electrostatic interactions.

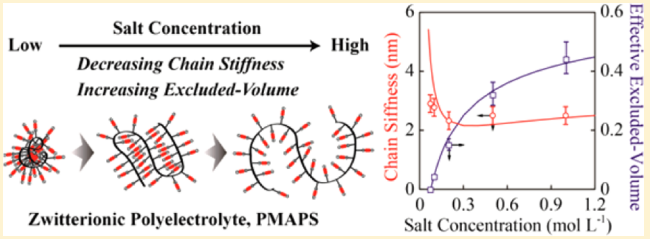

1. INTRODUCTION

Zwitterionic polyelectrolytes possessing both positively and negatively charged groups on the same monomer units or the pendent side chains of the different monomer units have received considerable attention[1−5] because they constitute many of natural substances such as poly(amino acid)s, proteins, DNA, and cell membrane surfaces. Polyzwitterion chains have exhibited a unique solution behavior in contrast with the conventional polyelectrolytes composed of the same sign charges. For the conventional polyelectrolytes the electrostatic forces between charged units are repulsive. The increase of added-salt concentration (C_s) results in the screening of the repulsive electrostatic forces between charged groups and the chain dimension for the polyelectrolytes in a dilute aqueous salt solution.[6] In contrast, the chain dimensions of the polyampholyte composed of both positively and negatively charged groups are thought to be determined by the competition between the repulsive and the attractive electrostatic forces. The net electrostatic forces of a neutral polyampholytes including the polyzwitterions due to the same number of positive and negative charges on the same chain show the attractive electrostatic interaction. Therefore, the polyzwitterions are usually insoluble in deionized water, but the chain dimensions of the polyzwitterions in a dilute aqueous salt solution increase with the increasing C_s because the attractive electrostatic forces between oppositely charged groups are reduced with the increasing C_s.

As in the case of a neutral polymer and the conventional polyelevtrolyte chains, the conformation of the polyampholyte chains is also conceivable to be determined by both short- and long-range interactions.[7,8] The former and latter interactions influence the chain stiffness parameter (Kuhn segment length λ^{-1}) and the excluded-volume effects, respectively. According to Ha and Thirumalai,[7] the λ^{-1} value for the polyampholyte chains is given by a sum of the intrinsic stiffness parameter (λ_0^{-1}) and the electrostatic chain stiffness parameter (λ_a^{-1}) arising from the charge fluctuations of an intrinsically polyampholyte. On the other hand, Higgs and Joanny reported that the effective excluded-volume parameter (λB, B is excluded-volume strength) for the polyampholyte chains is

Received: May 23, 2015
Revised: September 4, 2015
Published: September 14, 2015

DOI: 10.1021/acs.macromol.5b01116
Macromolecules 2015, 48, 7194−7204

also considered as a sum of the nonrepulsive ($\lambda_0 B_0$, B_0 is nonelectrostatic excluded-volume strength), the repulsive (β_e), and the attractive (β_a) electrostatic interactions.[8] The second (β_e) and third (β_a) terms are related to the contribution from the repulsive and the attractive electrostatic interactions between the positive and the negative monomers, so-called "the repulsive polyelectrolyte" and "the attractive polyampholyte" effects. Therefore, it is essential to investigate the ionic strength dependence of λ^{-1} and B for the zwitterionic polymer chains. However, it is extremely difficult to estimate separately the values of λ^{-1} and B for the zwitterionic polymer chains in the good solvent because both parameters are trade-off relationship. The most probable method to experimentally determine these factors separately is to thoroughly study the molecular weight dependence of the chain dimension for the flexible polyelectrolyte over a wide range of the molecular weight including oligomer and to analyze in terms of the Kratky−Porod (KP) wormlike cylinder model.[9,10]

Poly[3-(*N*-2-methacryloyloxyethyl-*N*,*N*-dimethyl)-ammonatopropanesulfonate] (PMAPS) is also a class of neutral polyampholytes and is to be thermosensitive and to present the upper critical solution temperature (UCST) dependent on both the polymer volume fraction and the degree of polymerization.[11−13] The unique ionic strength[12,14−19] and additive salt ion species[13,14,20] dependences of the chain dimensions for PMAPS in an aqueous solution have already been reported.[15,16] However, the experimental works for PMAPS in a dilute aqueous salt solution are limited to those with the molecular weight larger than 10^5 g mol^{-1} or broad molecular weight distribution. To determine the parameters of λ^{-1} and B as a function of C_s separately, PMAPS samples with the molecular weight lower than 10^4 g mol^{-1} and narrow molecular weight distribution are required because of the chain dimension of PMAPS is conceivable to be determined by the short-range interaction.

In this study, we were investigated the dimensional properties of PMAPS with a wide range of molecular weight including oligomer in aqueous NaCl solutions at 25 °C by small-angle X-ray scattering (SAXS), light scattering (LS), and viscometry, as shown in Figure 1. The PMAPS samples with

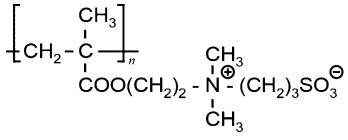

Figure 1. Chemical structure of PMAPS.

narrow molecular weight distribution (M_w/M_n = 1.07−1.19) were fractionated by a recycling preparative size-exclusion chromatography (SEC) system. The cylindrical wormlike chain model parameters for PMAPS in an aqueous NaCl solution were determined from the M_w dependences of the radius of gyration, the second virial coefficient, the interpenetration function, the hydrodynamic radius, and the intrinsic viscosity and SAXS profiles. The chain dimensional properties of PMAPS in aqueous NaCl solutions were studied and analyzed on the basis of the (un)perturbed cylindrical wormlike chain model to obtain the two parameters λ^{-1} and B. The C_s dependences of the values of λ^{-1} and B for PMAPS in aqueous NaCl solutions were compared with the theories for the polyampholytes.

2. EXPERIMENTAL SECTION

2.1. Materials. MAPS was synthesized and purified using previously reported procedures.[21] 2,2,2-Trifluoroethanol (TFE; Tokyo Chemical Inc., Japan) was used as received. The radical initiator 2,2′-azobis(isobutyronitrile) (AIBN; Wako Pure Chemicals, Japan) was purified by three recrystallizations from methanol. The PMAPS was prepared by free radical homopolymerization of MAPS monomer using AIBN as an initiator in TFE at 60 °C for 24 h. The reaction mixtures were poured into methanol to precipitate the polymer and to remove unreacted monomer. The obtained PMAPS was fractionated to 10 parts with the different size by a recycling preparative size exclusion chromatography (SEC) system (LC-9104; Japan Analytical Industry (JAI) Co., Ltd., Osaka, Japan) equipped with an refractive index (RI) detector (RI-7s; JAI) using two columns (GS620-50L and GS320-50L; JAI) in 0.2 M aqueous NaCl solution as an eluent at a flow rate of 20 cm^3 min^{-1} and room temperature. Deionized water (resistivity = 18.2 MΩ cm) for the all measurements was purified with arium 611UV (Sartorius Stedim Biotech GmbH, Göttingen, Germany). The fractionated aqueous solutions were concentrated in a rotary evaporator and then dialyzed against deionized water to remove salt. The aqueous solutions were poured into methanol to precipitate the fractionated samples and then dried in a vacuum at 40 °C for 12 h. The fractionated samples were dissolved in TFE and filtered three times through DISMIC filter units (polytetrafluoroethylene, pore size of 1.0 μm) to remove salt. The TFE solutions were concentrated in a rotary evaporator and then dried in a vacuum at 80 °C for 24 h. The values of C_s,[22] density (ρ_s),[22] refractive index (n_s),[18] and viscosity (η_s)[23] of an aqueous NaCl solution at 25 °C were calculated from previously reported equations.

2.2. Measurements. The values of the weight-average molecular weight (M_w), molecular weight distribution (M_w/M_n), *z*-average mean-square radius of gyration ($\langle S^2\rangle_z$), and intrinsic viscosity ([η]) for the fractionated PMAPS samples in aqueous NaCl solutions at C_s = 0.074, 0.10, 0.20, and 0.50 M were determined by SEC equipped with a multiangle light scattering (MALS) detector (DAWN-EOS; Wyatt Technology Co., Santa Barbara, CA, wavelength: λ = 690 nm) and a viscometer (ViscoStar; Wyatt Technology Co.) (SEC-MALS-Vis) at 25 °C. The SEC was carried out using a RI detector (RID-10A; Shimadzu Co., Kyoto, Japan) equipped with three columns (TSKgel G3000PW$_{XL}$, G5000PW$_{XL}$, and G6000PW$_{XL}$; Tosoh Co., Tokyo, Japan) in aqueous NaCl solutions at C_s = 0.074, 0.10, 0.20, and 0.5 M as an eluent at a flow rate of 0.8 cm^3 min^{-1} and column temperature of 40 °C. The Rayleigh ratio at a scattered angle of 90° was determined using a pure toluene.[24] The sensitivity and dead volume of 16 detectors were corrected using the scattering intensities of an aqueous NaCl solution of a poly[2-(*N*-2-methacryloyloxyethyl-*N*,*N*-dimethyl)-ammonatoethanesulfonate] with $M_w = 4.58 \times 10^4$ g mol^{-1} and M_w/M_n = 1.09. The standard polymer was prepared by atom transfer radical polymerization[25] and then fractionated by the recycling preparative SEC. The polymer solutions with mass concentration (C_p) of about 1×10^{-3} g cm^{-3} were injected using a sample loop of 100 μL to SEC columns and diluted down to 10−10^3 times lower than original C_p in the columns during the separation. Thus, the polymer concentration effect on the values of M_w, $\langle S^2\rangle_z$, and [η] can be ignored.[26] The values of the specific refractive index increment (dn/dc) and partial specific volume (ν_p) for PMAPS in aqueous NaCl solutions were used the previously reported values.[18] The angular dependence of the excess reduced scattering intensity was analyzed by using the Berry method.[27] The absolute calibration curve (circles) for PMAPS and SEC chromatograms of each PMAPS sample (P1 to P10) in 0.2 M aqueous NaCl solution are shown in Figure S1, together with $\langle S^2\rangle_z^{1/2}$ (squares) and [η] (diamonds) determined by SEC-MALS-Vis. The values of M_w and M_w/M_n were calculated from the absolute calibration curve.

Both SLS and DLS experiments of PMAPS in aqueous NaCl solutions at 25 °C were conducted at a scattering angle (θ) ranging from 30° to 150 ° using a goniometer system (ALV CGS-3-TAC/LSE-5004, Langen, Germany) with a He−Ne laser (λ = 632.8 nm, power of 22 mW). The Rayleigh ratio at a scattering angle of θ = 90° was based

DOI: 10.1021/acs.macromol.5b01116
Macromolecules 2015, 48, 7194−7204

Table 1. Molecular Characteristics of PMAPS Samples As Determined by SEC-MALS, SAXS, and SLS Measurements in Aqueous NaCl Solutions at 25 °C

			$\langle S^2\rangle_{z,0}^{1/2}$ (nm)				$A_2 \times 10^4$ [c] (g^{-2} mol cm^3)			
sample	$M_w \times 10^{-4}$ [a] (g mol^{-1})	M_w/M_n [a]	0.074 M	0.10 M	0.50 M	1.0 M	0.074 M	0.10 M	0.50 M	1.0 M
P1	0.550	1.07	1.37[b]							
P2	0.948	1.09	1.79[b]	1.78[b]	1.76[b]	1.77[b]	0.39	1.2	3.2	4.2
P3	1.82	1.12	2.54[b]	2.50[b]	2.51[b]	2.59[b]	0.02	0.40	2.1	2.5
P4	3.81	1.11	3.76[b]	3.67[b]	3.85[b]	3.96[b]	0	0.55	2.3	2.7
P5	8.69	1.13	5.83[b]	5.72[b]	5.96[b]	6.33[b]	0	0.52	1.6	1.9
P6	24.7	1.19	10.0[b]	9.91[b]	10.4[b]	12.2[b]	0	0.21	1.1	1.4
P7	41.3	1.12	12.6[b]	12.8[b]	15.0[c]	15.9[c]	0	0.38	1.0	1.1
P8	67.0	1.12	16.3[c]	17.0[c]	20.0[c]	22.1[c]	0	0.26	0.78	0.88
P9	102	1.13	20.2[c]	21.5[c]	26.1[c]	28.7[c]	0	0.12	0.72	0.88
P10	160	1.13	25.2[c]	27.1[c]	35.4[c]	38.1[c]	0	0.18	0.63	0.74

[a]Determined by SEC calibrated with a series of PMAPS's as a standard. [b]Determined by SAXS in aqueous NaCl solutions. [c]Determined by SLS in aqueous NaCl solutions.

on that of pure toluene at a wavelength of 632.8 nm at 25 °C.[24] The autocorrelation function ($g^{(2)}(t)$) at correlation time (t) was obtained by pseudo-cross-correlation of the signals from two photomultipliers to suppress noise. To determine the C_p values of the polymer solutions for the scattering experiments, we were used a gravimetric method instead of the simple method using volumetric flask including instrumental errors at a constant temperature (i.e., simply weighing polymer into a measuring volumetric flask and fill with solvent to the calibration mark). The preparation of polymer solutions by the former method are much more precise compared to that by the latter method and have been described elsewhere.[18] The weight fraction (W_p) was then converted to C_p by

$$C_p\ (\mathrm{g\,cm^{-3}}) = \frac{W_p}{\rho_s^{-1}(1 - W_p) + \upsilon_p W_p} \tag{1}$$

where υ_p is the partial specific volume of the polymer. The samples for SLS and DLS measurements had four different concentrations in aqueous NaCl solutions contained in cylindrical quartz cells with an inner diameter of 8 mm. The excess reduced scattering intensity (R_θ) obtained at θ was analyzed by means of Berry plot (see Figure S2),[27] i.e., $[KC_p/R_\theta]^{1/2}$ against $\sin^2(\theta/2)$ or C_p to obtain M_w, $\langle S^2\rangle_{z,0}^{1/2}$, and the second virial coefficient (A_2), where K denotes the optical constant. Details are described in the Supporting Information.

The typical $g^{(2)}(t) - 1$ and the relaxation spectrum ($A(\tau)$) measured by DLS for sample P8 in an aqueous NaCl solution at C_s = 1.0 M are shown in Figure S3. The values of M_w/M_n (1.07−1.19) for PMAPS samples fractionated by SEC were a little broad compared to those for standard polymer. Thus, the relaxation spectrum ($A(\tau)$) at relaxation time (τ) was calculated from the intensity $g^{(2)}(t) - 1$ at t by a CONTIN analysis.[28,29] The apparent diffusion coefficient (D_{app}) for each solution with finite C_p was evaluated from $A(\tau)$ using the following equations:

$$\Gamma = \frac{\sum_{i\in\mathrm{peak}} A(\tau_i)\tau_i^{-1}}{\sum_{i\in\mathrm{peak}} A(\tau_i)} \quad \text{where} \quad \sum_{i=0}^{\infty} A(\tau_i) = 1 \tag{2}$$

$$D_{app} = \lim_{q^2\to 0}(\Gamma q^{-2}) = D_0(1 + k_D C_p + \ldots) \tag{3}$$

where Γ, D_0, and k_D are the first cumulant, the diffusion coefficient at infinite dilution, and the concentration coefficient of the diffusion coefficient, respectively. The scattering vector (q) was defined as $4\pi n_s \sin(\theta/2)/\lambda$. Figure S4 shows plots of D_{app} against q^2 for sample P8 in 1.0 M aqueous NaCl solution. The value of D_{app} is almost independent of q^2, so that we adopt as the value of D_{app} at each finite C_p the mean value.[30] Figures S5−S8 show plots of D_{app} as a function of C_p for each sample of PMAPS (P1 to P10) in an aqueous NaCl solution at C_s = 0.074, 0.10, 0.5, and 1.0 M, respectively. Using the straight line fitting by least-square method for the D_{app} versus q^2, the values of D_0 and k_D can be determined from the intercept and the slope, respectively. From the values of the D_0 obtained from extrapolation of D_{app} to C_p = 0, the hydrodynamic radius (R_H) for each sample was evaluated by means of the equation

$$R_H = \frac{k_B T}{6\pi\eta_s D_0} \tag{4}$$

where k_B and T are the Boltzmann constant and the absolute temperature, respectively.

Synchrotron SAXS experiments of polymer solutions at 25 °C were carried out at the BL40B2 beamline of the SPring-8 facility (Hyogo, Japan) at an incident X-ray wavelength λ of 0.10 nm with a sample-to-detector distance of 2161 or 4136 mm. The scattering vector (q) defined as $4\pi \sin(\theta)/\lambda$, where 2θ is the scattering angle, was calibrated from the average of three peaks of the Bragg reflection of powdery silver behenate or nine peaks of dry collagen. The scattering intensity ($I(q)$) was detected by an imaging plate system (RAXIS VII; Rigaku Co., Tokyo, Japan) with 3000 × 3000 pixels to cover the range of scattering vectors from 0.04 to 3.5 nm^{-1}. The transmissivity (T) for the absorption of X-rays by a given solvent or solution was corrected by the ratio of the intensity of the X-rays beam transmitting the respective solvent or solution (I_1) to the intensity of the incident X-rays (I_0). The intensities of I_0 and I_1 were measured using the ion chamber. The sensitivity of the ion chambers was corrected using the scattering intensities of air. The excess scattering intensity ($\Delta I(q)$) was evaluated using the equation

$$\Delta I(q) = \frac{I(q)_{soln}}{I_{0,soln}T_{soln}} - \frac{I(q)_{solv}}{I_{0,solv}T_{solv}} \tag{5}$$

where the subscripts "soln" and "solv" for $I(q)$, I_0, and T signify those of the solution and the solvent. The solution of the sample was contained in a quartz capillary with an external diameter of 2 mm. To obtain the values of $[C_p/\Delta I(q)]_{Cp=0}$, the scattering intensities at each q were extrapolated to C_p = 0. The details are described elsewhere.[30] Figures S9−S12 show the Berry plots of $[C_p/\Delta I(q)]_{Cp=0}$ versus q^2 for each samples of PMAPS (P1 to P7) in aqueous NaCl solutions at C_s = 0.074, 0.10, 0.5, and 1.0 M, respectively. From the slope and the intercept of the solid line in Guinier region ($q^2 \ll 1/\langle S^2\rangle_z$) as shown in this figure, one determined the value of $\langle S^2\rangle_{z,0}^{1/2}$ for PMAPS in aqueous NaCl solutions at an infinite dilution by the following equation:

$$\left[\frac{C_p}{\Delta I(q)}\right]_{C_p=0}^{1/2} = \left[\frac{C_p}{\Delta I(0)}\right]_{C_p=0}^{1/2} + \frac{1}{6}\left[\frac{C_p}{\Delta I(0)}\right]_{C_p=0}^{1/2}\langle S^2\rangle_{z,0} q^2 + \ldots \tag{6}$$

The particle scattering function $[P(q)]$ is determined experimentally by the following equation:

DOI: 10.1021/acs.macromol.5b01116
Macromolecules 2015, 48, 7194−7204

$$\frac{1}{P(q)} = \frac{[C_p/\Delta I(q)]_{C_p=0}}{[C_p/\Delta I(0)]_{C_p=0}} \quad (7)$$

3. RESULTS AND DISCUSSION

Table 1 lists the characteristics of the fractionated PMAPS samples with M_w ranging from 5.50×10^3 to 1.60×10^6 g mol^{-1} and M_w/M_n ranging from 1.07 to 1.19 calculated from the absolute calibration curve of PMAPS. We fist report the theta salt concentration ($C_{s,\theta}$) for PMAPS in an aqueous NaCl solution at 25 °C. Second, the M_w dependences of the $\langle S^2\rangle_z$, A_2, the interpenetration function (Ψ), R_H, and $[\eta]$ and the C_s dependence of $P(q)$ for PMAPS are reported and analyzed on the basis of the cylindrical chain model to determine of the two parameters λ^{-1} and B. Third, the C_s dependences of the obtained λ^{-1} and B values for PMAPS in aqueous NaCl solutions are reported and compared with the theories for the polyampholyte.

3.1. Determination of Theta Salt Concentration. The Berry plots of $[KC_p/R(q)]_{q=0}^{1/2}$ versus C_p for PMAPS samples of P6 (upper) and P8 (lower) in aqueous NaCl solutions for a range from 0.050−0.10 M at 25 °C measured by SLS are shown in Figure 2a. From the slope and the intercept of the solid line in this figure, the values of M_w and A_2 for P6 and P8 in aqueous NaCl solutions were determined. The values of A_2 and M_w for the other PMAPS samples in aqueous NaCl solutions were also determined by the same method. The obtained M_w values determined by batch mode SLS using the ALV CGS-3-TAC were in agreement with that calculated from the absolute calibration curve of PMAPS within ±5%. Thus, we used the values of SEC-MALS for analysis of chain dimension. The obtained values of A_2 for PMAPS samples in aqueous NaCl solution at C_s = 0.074, 0.10, 0.50, and 1.0 M are summarized in Table 1. For the viewing clarity of C_s dependence of A_2, the plot of M_wA_2 versus $C_s^{1/2}$ for P6 (circles) and P8 (squares) in aqueous NaCl solutions at 25 °C is shown in Figure 2b. The values of M_wA_2 for both P6 and P8 samples are increased sharply with the increasing C_s. The value of M_wA_2 became 0 in an aqueous NaCl solution at C_s = 0.074 M. The values of A_2 for other PMAPS samples except for P2 and P3 (see also the subsection 3.3) almost vanish at a C_s of 0.074 M, as shown in Table 1. Therefore, we defined the θ-concentration ($C_{s,\theta}$) of PMAPS in an aqueous NaCl solution at 25 °C to be 0.074 M, which was slightly higher than previously reported value $C_{s,\theta}$ = 0.060 M at 30 °C by Kato et al.[16] The different might be caused by the purity of the PMAPS samples because hydrolysis of zwitterionic motives into acrylic acid naturally occurs during the radical polymerization of MAPS in water using ammonium persulfate as an initiator.[11,13]

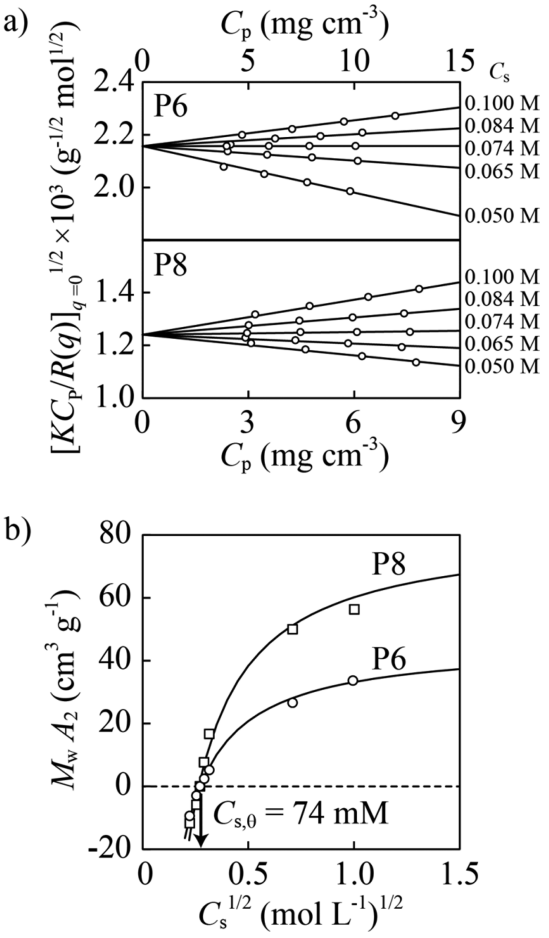

Figure 2. (a) Polymer concentration dependence of $[KC_p/R(q)]_{q=0}^{1/2}$ for PMAPS samples of P6 (upper) and P8 (lower) in aqueous NaCl solutions at 25 °C measured by SLS. (b) Dependence of M_wA_2 on $C_s^{1/2}$ for P6 (circles) and P8 (squares) in aqueous NaCl solutions. The solid curves connect the data points smoothly.

3.2. M_w Dependence of $\langle S^2\rangle$. Figure 3 shows the cross-section Guinier plots of $\ln[q\Delta I(q)/C_p]_{Cp=0}$ obtained by SAXS

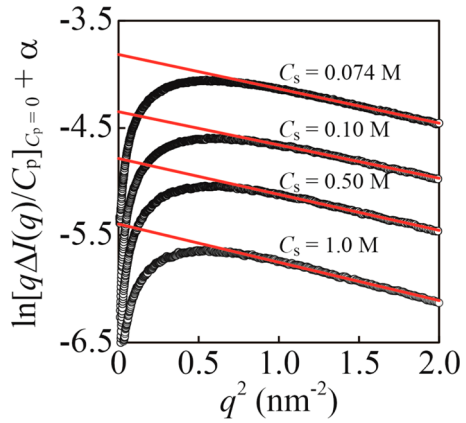

Figure 3. Cross-section Guinier plots of $\ln[q\Delta I(q)]_{Cp=0} + \alpha$ as a function q^2 for PMAPS sample of P2 in aqueous NaCl solutions at 0.074, 0.10, 0.50, and 1.0 M. The solid lines represent the initial slope within the cross-section Guinier region.

measurement against q^2 for P2 in aqueous NaCl solutions at C_s = 0.074, 0.10, 0.50, and 1.0 M. The cross-section mean-square radius of gyration ($\langle S_c^2\rangle$) at an infinite dilution for the PMAPS chain is determined from the initial slope of the solid line in Figure 3 within the cross-section Guinier region ($1/\langle S^2\rangle_z \ll q \ll 1/\langle S_c^2\rangle$) by using the following equation:[31]

$$\ln\left[q\frac{\Delta I(q)}{C_p}\right]_{C_p=0} = \ln\frac{k^2N\pi}{L} - \frac{1}{2}\langle S_c^2\rangle q^2 + \ldots \quad (8)$$

where L, k, and N are the contour length of the cylinder, the electron density contrast factor, and the number of cylinder, respectively. The values of $\langle S_c^2\rangle^{1/2}$ for P2 sample in 0.074, 0.10, 0.50, and 1.0 M aqueous NaCl solutions were estimated to be 0.80, 0.79, 0.82, and 0.84 nm. These values are summarized in

DOI: 10.1021/acs.macromol.5b01116
Macromolecules 2015, 48, 7194−7204

Table 2. Cylindrical Wormlike Chain Parameters of PMAPS in Aqueous NaCl Solutions

C_s (M)	$M_L \times 10^{-3}$ (g mol^{-1} nm^{-1})	λ^{-1} (nm)	$\langle S_c^2\rangle^{1/2}$ [a] (nm)	d_H (nm)	d_B (nm)	δ (nm)	B (nm)
0.074	1.15 ± 0.04	2.9 ± 0.3	0.80	1.9	1.35	0.35	0
0.10		2.8 ± 0.3	0.79	1.9	1.35		0.12
0.20		2.3 ± 0.3			1.35		0.35
0.50		2.5 ± 0.3	0.82	1.9	1.35		0.80
1.0		2.5 ± 0.3	0.84	1.9			1.1

[a]Determined by SAXS in aqueous NaCl solutions.

Table 2 and are almost constant over the entire C_s region from 0.074 to 1.0 M.

The values of smaller $\langle S^2\rangle_{z,0}^{1/2}$ (<15 nm) for PMAPS in aqueous NaCl solutions were determined by SAXS, whereas those of larger $\langle S^2\rangle_{z,0}^{1/2}$ (≥15 nm) for PMAPS were determined by SLS. The values of $\langle S^2\rangle_{z,0}^{1/2}$ for PMAPS samples in aqueous NaCl solutions at C_s = 0.074, 0.10, 0.50, and 1.0 M obtained from SAXS and SLS are listed in Table 1. The values of retention volume (RV), M_w, and $\langle S^2\rangle_z^{1/2}$ for PMAPS with the high M_w (>6.49 × 10^5 g mol^{-1}) in aqueous NaCl solutions at C_s = 0.074, 0.10, 0.20, and 0.50 M determined by SEC-MALS are listed in Table S1. Figure 4

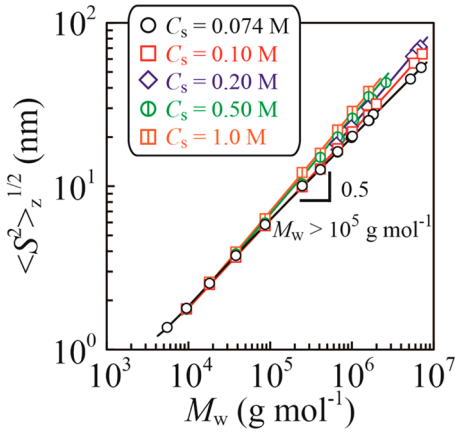

Figure 4. M_w dependence of the measured $\langle S^2\rangle_z^{1/2}$ for PMAPS in aqueous NaCl solutions. The solid lines represent the theoretical values calculated from eqs 9−11 and 13−16 using the parameters λ^{-1}, M_L, δ, $\langle S_c^2\rangle$, and B.

shows the M_w dependence of double-logarithmic plots of the measured $\langle S^2\rangle_z^{1/2}$ against M_w for PMAPS in 0.074, 0.10, 0.20, 0.50, and 1.0 M aqueous NaCl solutions, together with those for PMAPS with high M_w determined by SEC-MALS listed in Table S1. We found that 0.074 M aqueous NaCl solution with M_w > 10^5 g mol^{-1} reveals the scaling exponent to be 0.5 from the slope of double-logarithmic plots of $\langle S^2\rangle_z^{1/2}$ against M_w, as shown in this figure. The slopes of double-logarithmic plots of $\langle S^2\rangle_z^{1/2}$ against M_w at other C_s are 0.55 for C_s = 0.10 M, 0.58 for C_s = 0.20 M, 0.65 for C_s = 0.5 M, and 0.62 for C_s = 1.0 M. The slopes increase from 0.5 at C_s = 0.074 M to 0.65 at C_s = 0.50 M. An interesting and remarkable observation to be noted in this figure and Table 1 is that the values of $\langle S^2\rangle_z^{1/2}$ for M_w > 1.9 × 10^4 g mol^{-1} increase with the increasing C_s, but those for M_w < 1.9 × 10^4 g mol^{-1} almost constant over the entire C_s region from 0.074 to 1.0 M within experimental error. The former phenomenon is the same as the previous studies for PMAPS[15,16] such as called antipolyelectrolyte solution behavior, whereas the latter phenomenon implies that the local conformation of PMAPS is not almost change. For the unperturbed KP chain,[32] the continuous change in conformation from rodlike (scaling exponent of 1) to Gaussian (scaling exponent of 0.5) chains with the increasing molecular weight can be expected. However, such a trend can hardly be seen in Figure 4, despite that even extremely short chains have been included in this study. It is possible that the difference in the scaling exponent between the predictive value in the rod limit of short chains and the experimental value (0.52 for M_w < 2.0 × 10^4 g mol^{-1}) could be attributed to the same order magnitude of the values of λ^{-1} and the chain diameter. To confirm the continuous change in conformation of PMAPS chains, we used the ρ parameter. It is well-known that ρ, defined as the ratio of the $\langle S^2\rangle_{z,0}^{1/2}$ to the R_H, is a universal constant and sensitive to shape of polymer chains. The M_w dependence of ρ value for PMAPS in an aqueous NaCl solution at C_s = 0.074 M is shown in Figure S13. One sees in this figure that the experimental ρ value increases with the increasing M_w and then leveled off at 1.31 for above log M_w = 5.5, similar to that observed for a bottle brush polymer with relatively low M_w in theta solvent.[33] This clearly implies that the simple KP chain model is not applicable to describe the dependence of $\langle S^2\rangle_z^{1/2}$ on M_w.

One analyzes the dependence of $\langle S^2\rangle_z^{1/2}$ on M_w for PMAPS at $C_{s,\theta}$, based on the cylindrical wormlike chain model with an end effect.[34] This situation is schematically shown in Figure 5,

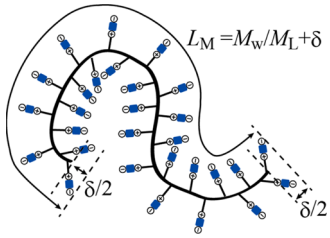

Figure 5. Schematic cartoon of the end effects of side chains (δ) near the ends on the main chain contour of the PMAPS.

in which $\delta/2$ stands for the contribution of side chains near the ends to the main chain contour. The main chain contour length (i.e., L_M) may be given by

$$L_M = \frac{M}{M_L} + \delta \tag{9}$$

where M_L is the molecular weight per unit contour length. The mean-square radius of gyration ($\langle S^2\rangle$) for a cylindrical wormlike chain may be expressed by[35]

$$\langle S^2\rangle = \langle S_M^2\rangle + \langle S_c^2\rangle \tag{10}$$

where $\langle S_M^2\rangle$ is the main chain mean-square radius of gyration of a polymer chain having a contour length L_M. According to Benoit and Doty for the KP chain,[32] the unperturbed $\langle S_M^2\rangle$ of a monodispersed wormlike chain with L_M is expressed by

DOI: 10.1021/acs.macromol.5b01116
Macromolecules 2015, 48, 7194−7204

$$\langle S_M{}^2\rangle = \frac{L_M}{6\lambda} - \frac{1}{4\lambda^2} + \frac{1}{4\lambda^3 L_M} - \frac{1}{4\lambda^4 L_M{}^2}[1 - \exp(-2\lambda L_M)] \quad (11)$$

Equation 11 may be approximated by a straight line according to[26,36]

$$\left(\frac{M}{\langle S_M{}^2\rangle}\right)^{1/2} = (6\lambda M_L)^{1/2}\left[1 + \frac{3M_L}{2}\left(\frac{1}{2\lambda} - \frac{\delta}{3}\right)\frac{1}{M}\right] \quad (12)$$

with the maximum error from the exact value being 2% for $\lambda L_M > 4$. Equation 12 (denoted as the modified Murakami plot) enables evaluation of the two parameters λ^{-1} and M_L form the intercept and initial slope the plot of $(M/\langle S_M{}^2\rangle)^{1/2}$ versus M^{-1} with a fitting parameter δ. Figure 6 shows the modified

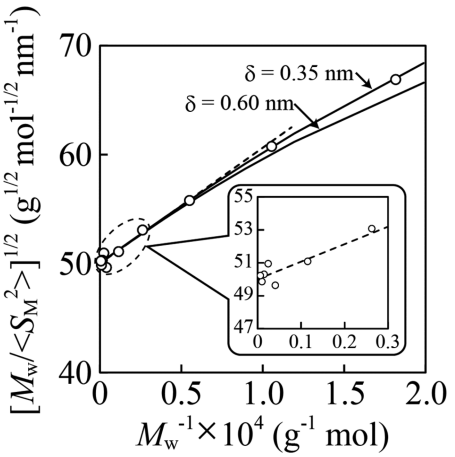

Figure 6. Modified Murakami plots of $[M_w/\langle S_M{}^2\rangle]^{1/2}$ versus $M_w{}^{-1}$ for PMAPS in 0.074 M aqueous NaCl solution. The broken line shows a linear region, and solid curves are theoretical values recalculated from eqs 9−11 using the indicated δ value. The marked region is enlarged in the inset.

Murakami plots constructed from the experimental data for PMAPS in an aqueous NaCl solution at $C_{s,\theta}$ = 0.074 M. From the data points within a linear region ($\lambda L_M > 4$), the values of the slope and intercept of the broken line as shown in this figure were determined to be 1.06×10^5 g$^{3/2}$ mol$^{-3/2}$ nm^{-1} and 50.0 g$^{1/2}$ mol$^{-1/2}$ nm^{-1}, respectively. The values of M_L and λ^{-1} were calculated from eq 12 using the obtained slope and intercept to be 1090 g mol^{-1} nm^{-1} and 2.61 nm for δ = 0 nm, 1140 g mol^{-1} nm^{-1} and 2.73 nm for δ = 0.35 nm, and 1170 g mol^{-1} nm^{-1} and 2.81 nm for δ = 0.60 nm. The solid curves in this figure are the theoretical values recalculated from eqs 9−11 with the indicated δ values. The experimental data for PMAPS at $C_{s,\theta}$ were in agreement with the theoretical values using the three parameters of λ^{-1} = 2.73 nm, $M_L = 1.14 \times 10^4$ g mol^{-1} nm^{-1}, and δ = 0.35 nm. In Figure 4, the comparison of the experimental data of PMAPS at $C_{s,\theta}$ with the theoretical curve (black line), calculated by using eqs 9−11 with the model parameters λ^{-1} = 2.73 nm, $M_L = 1.14 \times 10^3$ g mol^{-1} nm^{-1}, $\langle S_c{}^2\rangle^{1/2}$ = 0.80 nm, and δ = 0.35 nm, is shown. It can be seen that the experimental M_w dependence of $\langle S^2\rangle_{z,0}{}^{1/2}$ in an aqueous NaCl solution at $C_{s,\theta}$ = 0.074 M is quantitatively described by the unperturbed wormlike cylinder model with the end effect.

Since aqueous NaCl solutions at greater C_s region than 0.074 M are good solvent for PMAPS, we take into account the intramolecular excluded-volume effects on the radius of gyration. In the following, we analyzed the experimental $\langle S^2\rangle_z{}^{1/2}$ values with the aid of quasi-two-parameter (QTP) theory[37−39] for the KP chain. In the QTP scheme, the radius expansion factor $\alpha_S = (\langle S^2\rangle/\langle S_M{}^2\rangle)^{1/2}$ is a universal function of the scaled excluded-volume parameter ($\tilde{z}$) defined by

$$\tilde{z} = \frac{3}{4}K(\lambda L_M)z \quad (13)$$

with

$$z = \left(\frac{3}{2\pi}\right)^{3/2}(\lambda B)(\lambda L_M)^{1/2} \quad (14)$$

and

$$K(\lambda L_M) = \frac{4}{3} - 2.711(\lambda L_M)^{-1/2} + \frac{7}{6}(\lambda L_M)^{-1} \quad \text{for } \lambda L_M > 6$$
$$= (\lambda L_M)^{-1/2}\exp[-6.611(\lambda L_M)^{-1} + 0.9198 + 0.03516(\lambda L_M)] \quad \text{for } \lambda L_M \le 6 \quad (15)$$

where z is the conventional exclude-volume parameter and B is the excluded-volume strength defined by $B = \beta/a_B{}^2$ with β and a_B being the binary cluster integral representing the interaction between a pair of beads and the bead spacing, respectively. Adopting the Domb−Barrett equation[40] for $\alpha_S{}^2$, we have following equation:

$$\alpha_S{}^2 = \left[1 + 10\tilde{z} + \left(\frac{70\pi}{9} + \frac{10}{3}\right)\tilde{z}^2 + 8\pi^{3/2}\tilde{z}^3\right]^{2/15} \times [0.933 + 0.067\exp(-0.85\tilde{z} - 1.39\tilde{z}^2)] \quad (16)$$

Since the determination of λ^{-1}, M_L, δ, and B by the way mentioned above is considerably difficult, one fixed two model parameters ($M_L = 1.14 \times 10^3$ g mol^{-1} nm^{-1} and δ = 0.35 nm) estimated from $\langle S^2\rangle_z$ at $C_{s,\theta}$. The comparison of the experimental data of PMAPS in aqueous NaCl solutions for a range from 0.10 to 1.0 M with the best-fit theoretical curves (solid lines) calculated from eqs 9−11 and 13−16 using the model parameters (λ^{-1}, M_L, δ, and B) and obtained $\langle S_c{}^2\rangle$ is shown in Figure 4. The values of λ^{-1} and B are estimated to be 2.5 and 0.12 nm for 0.1 M, 2.2 and 0.35 nm for 0.2 M, 2.2 and 0.80 nm for 0.50 M, and 2.2 nm and 1.1 nm for 1.0 M. The B values at all C_s are summarized in Table 2.

3.3. M_w Dependences of A_2 and Ψ. Figure 7 shows double-logarithmic plots of the obtained values of A_2 against M_w for PMAPS in 0.074, 0.10, 0.50, and 1.0 M aqueous NaCl solutions. It is seen that for 0.074 M aqueous NaCl solution at $C_{s,\theta}$ A_2 is definitely positive in the range displayed and increases steeply with the decreasing M_w. For good solvents at other C_s, the values of A_2 increase with the decreasing M_w and the increasing C_s, more steeply for smaller M_w. All these steep increases of A_2 are in qualitative agreement with the results[41] of polystyrene in the theta (cyclohexane at 34.5 °C) and good (toluene at 15.0 °C) solvents. The analysis of A_2 may be regarded as arising from the effect of chain ends. We analyze the M_w dependence of the A_2 value for PMAPS by the use of the Yamakawa theory[42] which considers the effect of chain ends on the basis of the helical wormlike (HW) touched-bead model. The A_2 value is given by a sum of the part of A_2 without the effect of chain ends ($A_2{}^{(HW)}$) and that with the effects of chain ends ($A_2{}^{(E)}$). The first term $A_2{}^{(HW)}$ vanishes at the theta state and may be expressed by

DOI: 10.1021/acs.macromol.5b01116
Macromolecules 2015, 48, 7194−7204

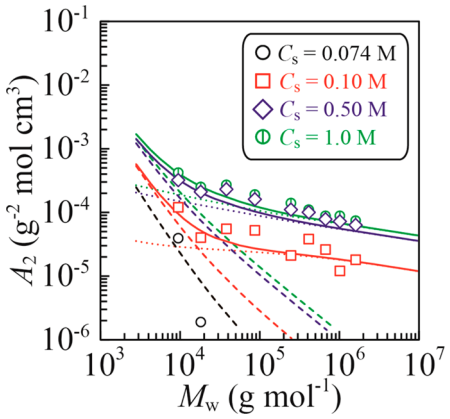

Figure 7. M_w dependence of the observed values of A_2 for PMAPS in aqueous NaCl solutions at C_s = 0.074, 0.10, 0.50, and 1.0 M. The solid curves represent the theoretical values of A_2; the dotted and dashed curves represent those of $A_2^{(HW)}$ and $A_2^{(E)}$, respectively.

$$A_2^{(HW)} = \frac{N_A C_\infty{}^{3/2} L_M{}^2 B}{2M^2} h(\hat{z}) \tag{17}$$

where N_A is Avogadro's number and C_∞ is the HW model parameter defined as $(4 + \tau_0{}^2)/(4 + \kappa_0{}^2 + \tau_0{}^2)$, where κ_0 and τ_0 are the constant curvature and the torsion of the characteristic regular helix at the energy minimum. The HW chain in a special case of $\kappa_0 = 0$ corresponds to the KP chain. Thus, the value of C_∞ for the KP chain is equal to 1. The $h(\hat{z})$ function is given by eqs 14−16 and eqs S3−S6. The second term $A_2^{(E)}$ may be expressed by

$$A_2^{(E)} = \frac{2N_A\beta_1}{M_0} M^{-1} + 2N_A(\beta_2 - 2\beta_1)M^{-2} \tag{18}$$

where β_1 and β_2 are the excess effective binary cluster integrals associated with one and two end beads, respectively. Equation 18 indicates that $A_2^{(E)}M$ plotted against M^{-1} should give a straight line whose the slope and the intercept allow one the two parameters β_1 and β_2 to be evaluated. In the case of solutions at the theta state, the experimental A_2 value is equal to $A_2^{(E)}$ because of $A_2^{(HW)} = 0$ ($\beta = 0$). However, in the case of in the good solvent, we must subtract the theoretical value of $A_2^{(HW)}$ from the experimental value of A_2 to obtain $A_2^{(E)}$. The $A_2^{(HW)}$ values in good solvents were calculated from eqs 14−17 and eqs S3−S6 with the values of the model parameters (λ^{-1}, M_L, δ, and B) determined from $\langle S^2\rangle_z$.

Figure S14 shows plots of $A_2^{(E)}M_w$ against $M_w{}^{-1}$ for the PMAPS in aqueous NaCl solutions at C_s = 0.074, 0.10, 0.5, and 1.0 M. The two data points are fitted by a straight line, as shown in this figure. From the slope and the intercept of straight line, the values of β_1 and β_2 were calculated from eq 18 to be 0.012 nm^3 and 1.5 nm^3 for 0.074 M, 0.058 nm^3 and 3.0 nm^3 for 0.10 M, 0.23 nm^3 and 6.1 nm^3 for 0.50 M, and 0.30 nm^3 and 6.8 nm^3 for 1.0 M, respectively. The obtained values of β_1 and β_2 increase with the increasing C_s. The value of β_1 for the PMAPS in aqueous NaCl solutions is in agreement with that for polystyrene in the theta (0.016 nm^3) and good (0.22 nm^3) solvents, whereas the values of β_2 is 1 order of magnitude lager than that for polystyrene in the theta (0.26 nm^3) and good (0.27 nm^3) solvents.[41]

The comparison of the experimental data of PMAPS in aqueous NaCl solutions for a range from 0.074 to 1.0 M with the theoretical values of $A_2^{(HW)} + A_2^{(E)}$ (solid curves) calculated from eqs 14−18 and eqs S3−S6 with the values of all necessary parameters determined, as mentioned above, is shown in Figure 7. The theoretical contributions of $A_2^{(HW)}$ and $A_2^{(E)}$ are shown by the dotted and dashed curves, respectively. Although the data points in 0.074 and 0.1 M aqueous NaCl solutions somewhat scatter, they are in relative agreement with the theoretical values. The obtained values of A_2 in 0.5 and 1.0 M for $M_w > 3 \times 10^4$ g mol^{-1} are somewhat larger than the theoretical ones. The different may be regarded as arising from the fact that the theoretical $h(\hat{z})$ function is underestimated except for very large z, similar to that for polystyrene in good solvent.[41]

We discuss in terms of dimensionless interpenetration function. According to Einaga et al., the true interpenetration function (Ψ) from the obtained values of A_2 including the contribution $A_2^{(E)}$ of the effect of chain ends should be defined by[41]

$$\psi = \frac{[A_2 - A_2^{(E)}]M^2}{4\pi^{3/2} N_A \langle S_M{}^2\rangle^{3/2}} \tag{19}$$

Figure 8 shows the plots of the value of Ψ calculated from eq 19 versus the root-reduced contour length $[(\lambda L_M)^{1/2}]$ for

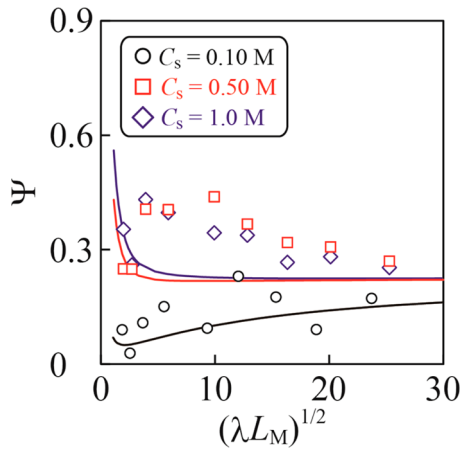

Figure 8. Plots of Ψ versus $(\lambda L_M)^{1/2}$ for PMAPS in aqueous NaCl solutions at C_s = 0.10, 0.50, and 1.0 M. The solid curves represent the theoretical values calculated from eqs 9, 11, and 14−16 and eqs S3−S6.

PMAPS in the good solvents (C_s = 0.10, 0.50, and 1.0 M). The value of Ψ in a 0.10 M aqueous NaCl solution slightly increases with the increasing $(\lambda L_M)^{1/2}$, whereas that in 0.5 and 1.0 M for $M_w > 2 \times 10^4$ g mol^{-1} decreases with the increasing $(\lambda L_M)^{1/2}$. The solid curves represent the theoretical values of Ψ calculated from[42]

$$\psi = \left(\frac{C_\infty \lambda L_M}{6\lambda^2 \langle S^2\rangle_{KP}}\right)^{3/2} \left(\frac{z}{\alpha_s{}^3}\right) h(\hat{z}) \tag{20}$$

with eqs 9, 11, and 14−16 and eqs S3−S6 using the values of the parameters given above. Although the data points in 0.1 M aqueous NaCl solutions somewhat scatter, they are in relative agreement with the theoretical values. The experimental values of Ψ for PMAPS in 0.5 and 1.0 M aqueous NaCl solutions except for two data points of low molecular region ($M_w < 2 \times 10^4$ g mol^{-1}) are somewhat larger than that of the theoretical values, similar to the M_w dependence of A_2 at the same C_s.

DOI: 10.1021/acs.macromol.5b01116
Macromolecules 2015, 48, 7194−7204

3.4. M_w Dependence of R_H. The values of R_H and k_D for PMAPS samples in aqueous NaCl solutions at C_s = 0.074, 0.10, 0.50, and 1.0 M obtained from DLS are listed in Table S2. Figure 9 shows the double-logarithmic plots of R_H versus M_w

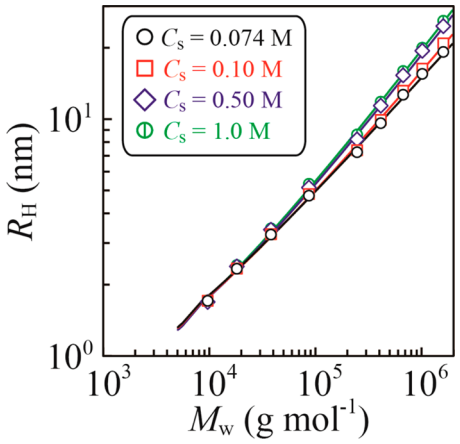

Figure 9. M_w dependence of the measured R_H for PMAPS in aqueous NaCl solutions. The solid lines are the theoretical values calculated from eqs 9, 13−15, 21, 49−52 of ref 43 and eqs 22, 23 of ref 44 using the parameters λ^{-1}, M_L, δ, d_H, and B.

for PMAPS in aqueous NaCl solutions at C_s = 0.074, 0.10, 0.50, and 1.0 M. It is seen that the values of R_H for $M_w > 1.9 \times 10^4$ g mol^{-1} increase with the increasing C_s, but those for $M_w < 1.9 \times 10^4$ g mol^{-1} almost constant within experimental error. This phenomenon is the same as the M_w dependence of $\langle S^2 \rangle_z$. We analyze the M_w dependence of R_H for PMAPS based on the following theories. Yamakawa−Fujii theory[43] for the translational friction coefficient allows us to calculate R_H for unperturbed cylinders as functions of λL_M and λd_H, where d_H is the hydrodynamic chain diameter. This theory is, however, valid only for L_M/d_H larger than about 4 because it does not consider the frictional force from the cylinder ends. This end effects is taken into consideration in the theory of Norisuye et al.[44] for wormlike cylinders with hemispheres at both ends, but the theory is applicable only to small L/d_H. The excluded-volume effects are considered by multiplying $R_{H,0}$ by the hydrodynamic radius expansion factor α_H, which may be by calculated from the following modified Barrett equation:[45]

$$\alpha_H = (1 + 6.09\tilde{z} + 3.59\tilde{z}^2)^{0.1} \tag{21}$$

For PMAPS at $C_{s,\theta}$, the best-fit theoretical value (black curve in Figure 9) calculated from eqs 9, 49−52 of ref 43 and eqs 22, 23 of ref 44 was obtained when we used the model parameters λ^{-1} (3.2 nm), M_L (1.11×10^3 g mol^{-1} nm^{-1}), δ (0.35 nm), and d_H (1.9 nm). For PMAPS in good solvents, we fixed two model parameters (M_L and d_H) estimated from R_H at $C_{s,\theta}$ and values of δ and B determined from $\langle S^2 \rangle_z$ listed in Table 2. The comparison of the experimental data of PMAPS in aqueous NaCl solutions at C_s = 0.10, 0.50, and 1.0 M with the best-fit theoretical curves (solid lines) calculated from eqs 9, 13−15, 21, 49−52 of ref 43 and eqs 22, 23 of ref 44 using the fitting parameter λ^{-1} (3.1 nm for 0.1 M, 2.8 nm for 0.50 M, and 2.8 nm for 1.0 M) shown in Figure 9. The obtained value of d_H is listed in Table 2.

3.5. M_w Dependence of $[\eta]$. The values of RV, M_w, and $[\eta]$ for PMAPS samples in aqueous NaCl solutions at C_s = 0.074, 0.10, 0.20, and 0.5 M obtained from SEC-MALS-Vis are listed in Table S3. Figure 10 shows the double-logarithmic plots of $[\eta]$ against the M_w for PMAPS in aqueous NaCl solutions at

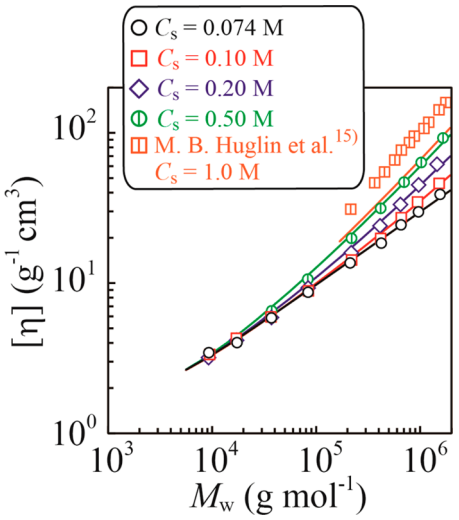

Figure 10. M_w dependence of the measured $[\eta]$ for PMAPS in aqueous NaCl solutions together with that[15] for PMAPS in 1.0 M aqueous NaCl solution. The solid lines are the theoretical values calculated from eqs 9, 11, 13−15, 22−24 and eqs 22, 25, 26 of ref 46 using the coefficients listed in Table 1 of ref 46 and the parameters λ^{-1}, M_L, δ, d_B, and B.

C_s = 0.074, 0.10, 0.20, and 0.50 M. It is seen that the values of $[\eta]$ for $M_w > 1.9 \times 10^4$ g mol^{-1} increase with the increasing C_s, but those for $M_w < 1.9 \times 10^4$ g mol^{-1} almost constant within experimental error, similar to the M_w dependences of $\langle S^2 \rangle_z$ and R_H. We analyze the M_w dependence of the $[\eta]$ value for PMAPS based on the following theory. According to the theory of Yoshizaki et al.[46] for the touched-bead chain model composed of N beads of diameter d_B ($L_M = Nd_B$), the unperturbed intrinsic viscosity ($[\eta]_0$) is expressed as the sum of the solution ($[\eta]_{KR}$) of the Kirkwood−Riseman type equation[47] and the contribution ($[\eta]_E$) of the Einstein spheres

$$[\eta]_0 = [\eta]_{KR} + \frac{L_M}{d_B}[\eta]_E \tag{22}$$

and

$$[\eta]_E = \frac{5\pi N_A d_B^3}{12M} \tag{23}$$

The excluded-volume effects are considered by multiplying $[\eta]_0$ by the intrinsic viscosity expansion factor α_η^3, which may be calculated from the following modified Barrett equation:[48]

$$\alpha_\eta^3 = (1 + 3.8\tilde{z} + 1.9\tilde{z}^2)^{0.3} \tag{24}$$

For PMAPS at $C_{s,\theta}$, the best-fit theoretical value (black curve in Figure 10) calculated from eqs 9, 11, 22, 23 and eqs 22, 25, 26 of ref 46 using the coefficients listed in Table 1 of ref 46 was obtained when we used the model parameters λ^{-1} (2.6 nm), M_L (1.19×10^3 g mol^{-1} nm^{-1}), δ (0.35 nm), and d_B (1.35 nm). For PMAPS in good solvents, we fixed two model parameters (M_L and d_B) estimated from $[\eta]$ at $C_{s,\theta}$ and values of δ and B determined from $\langle S^2 \rangle$ listed in Table 2. The solid lines in Figure 10 are the best-fit theoretical values calculated from eqs 9, 11, 13−15, 22−24 and eqs 22, 25, 26 of ref 46 using the fitting parameters λ^{-1} (2.5 nm for 0.10 M, 2.4 nm for 0.20 M,

DOI: 10.1021/acs.macromol.5b01116
Macromolecules 2015, 48, 7194−7204

and 2.3 nm for 0.5 M) and the coefficients listed Table 1 of ref 46. The obtained value of d_B is listed in Table 2. As mentioned above, we have already confirmed that the model parameters (λ^{-1} = 2.2 nm, M_L = 1.19 × 10^3 g mol^{-1} nm^{-1}, δ = 0.35 nm, and B = 1.1 nm) of PMAPS in 1.0 M aqueous NaCl solution are identical to M_w dependence of $\langle S^2\rangle^{1/2}$ and R_H. We can therefore compare the theoretical values calculated from touched-bead chain model using our present model parameters with the literature data. The literature values[15] of $[\eta]$ for PMAPS in an aqueous NaCl solution at C_s = 1.0 M are plotted in Figure 10. The slight difference between our study and previous data might be attributed to a broad polydispersity compared with our experiment.

Although the values of M_L and λ^{-1} for PMAPS estimated from $\langle S^2\rangle_z$, R_H, and $[\eta]$ somewhat scatter, they are almost constant within experimental error. These mean values and the experimental errors are summarized in Table 2. The contour length per backbone monomer (l_M) calculated from $l_M = M_0/M_L$ (M_0 is molecular mass of PMAPS) was 0.24 ± 0.1 nm, which is similar to that of poly(methyl methacrylate) (PMMA) chain with the *all-trans* conformation. The experimental value of λ^{-1} for PMAPS in an aqueous NaCl solution decreases barely and then constant with increasing C_s, whereas the value of B increase gradually with C_s. Thus, there results allow one to conclude that the dominant factor to determine the chain dimension of PMAPS in an aqueous NaCl solution is considered the long-range interaction (i.e., B).

3.6. C_s Dependence of $P(q)$ for P2. To demonstrate the validity of the model parameters determined from the M_w dependence of $\langle S^2\rangle_z$, R_H, and $[\eta]$ for PMAPS in aqueous NaCl solutions at C_s = 0.074, 0.10, 0.5, and 1.0 M, we confirmed whether the cylindrical wormlike chain model can be described by $P(q)$ with the model parameters. The numbers of Kuhn's segment ($n_K = \lambda L_M$) for sample P2 in good solvents are 3.0 ± 0.4 for 0.1 M and 3.4 ± 0.5 for 0.5 and 1.0 M. According to Norisuye et al.,[49] the intramolecular excluded-volume effects in this region substantially disappear. Thus, the theories of Yamakawa et al.[50,51] for an unperturbed wormlike chain with a circular cross section are applied in present study for describing $P(q)$. Figure 11 shows the scattering profiles, $q^2P(q)$ against the magnitude q of the scattering vector (in the form of Kratky plot) for sample P2 in aqueous NaCl solutions at C_s = 0.074, 0.10, 0.5, and 1.0 M. The solid curves are the best-fit theoretical values calculated from eqs 9, 11, 13−23 of ref 50 and eqs 50−52 of ref 51 using the two fitting parameters (M_L and λ^{-1}), the values ($\langle S_c^2\rangle$ and δ) listed in Table 2, and the coefficients listed in Table 1 of ref 50. The values of M_L and λ^{-1} are estimated to be 1.18 × 10^3 g mol^{-1} and 2.9 nm for 0.074 M, 1.17 × 10^3 g mol^{-1} and 2.6 nm for 0.10 M, 2.2 nm, 1.16 × 10^3 g mol^{-1}, and 2.6 nm for 0.50 M, and 1.12 × 10^3 g mol^{-1} and 2.7 nm for 1.0 M. These parameters are in agreement with those determined from $\langle S^2\rangle_z$, R_H, and $[\eta]$ listed in Table 2.

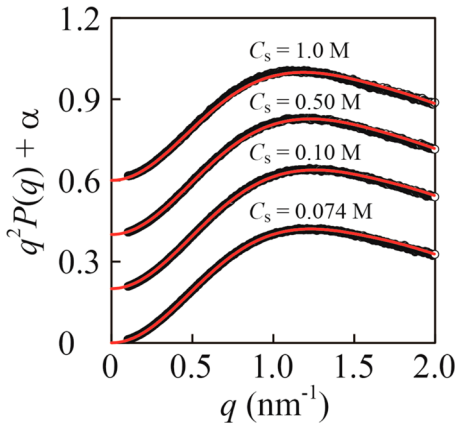

Figure 11. Kratky plots for PMAPS (P2) in aqueous NaCl solutions at C_s = 0.074, 0.10, 0.50, and 1.0 M. The solid lines are the theoretical values calculated from eqs 9, 11, 13−23 of ref 50 and eqs 50−52 of ref 51 using the parameters λ^{-1}, M_L, δ, and $\langle S_c^2\rangle$.

3.7. C_s Dependence of λ^{-1} and B. The C_s dependence of λ^{-1} for PMAPS in an aqueous NaCl solution at 25 °C is shown in Figure 12. One sees in this figure that the experimental λ^{-1} decreases barely but is almost constant with the increasing C_s. According to Ha and Thirumalai, the C_s dependence of the chain stiffness for the polyampholyte chains is predicted by the following equation:[7]

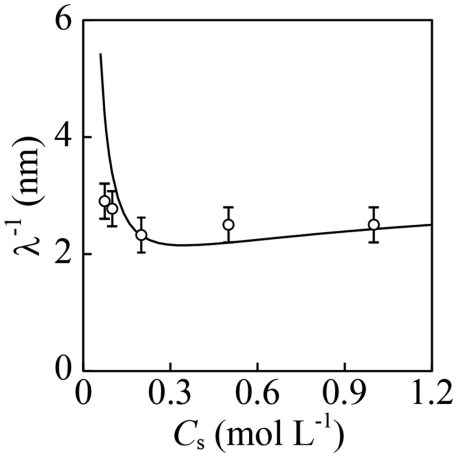

Figure 12. Comparison of C_s dependence of the experimental values of λ^{-1} for PMAPS in aqueous NaCl solutions with theoretical curve (solid line) calculated from eq 25 using l_M = 0.24 nm, λ_0^{-1} = 4.2 nm, and b = 1.8.

$$\lambda^{-1} = \lambda_0^{-1} + \frac{l_B}{2l_M^2\kappa^2} - \frac{l_B^2 b^2}{4l_M^2\kappa} \qquad (25)$$

where λ_0^{-1} is the intrinsic chain stiffness parameter, l_B is the Bjerrum length defined by $l_B = e^2/\varepsilon k_B T$ equal to 0.714 nm for water at 25 °C (e and ε denote the elementary charge and the dielectric constant of the solvent), κ^{-1} is the Debye−Hückel screening length defined by $\kappa^2 = 8\pi l_B N_A C_s/1000$, and b is the charge fluctuation parameter. For homogeneously charged chains (b = 0), this equation correspond to that of OSF theory.[52,53] The solid line in Figure 12 represents the theoretical values calculated from eq 25 using the fitting parameters of λ_0^{-1} = 3.8 nm and b = 1.7. The experimental C_s dependence of λ^{-1} for PMAPS in aqueous NaCl solutions was in good agreement with the theoretical value. The value of λ_0^{-1} of PMAPS is larger than that (1.42 nm[54]) of PMMA. It is possible that the difference in the value of λ_0^{-1} between PMAPS and PMMA can be attributed to the repulsive interaction of the side chains because the chain diameter (see Table 2) of PMAPS is longer than that (d_B = 0.72−0.79 nm,[55] d_H = 0.99 nm[56]) of PMMA.

Figure 13 shows a C_s dependence of λB for PMAPS in aqueous NaCl solution at 25 °C. It should be noted that the

DOI: 10.1021/acs.macromol.5b01116
Macromolecules 2015, 48, 7194−7204

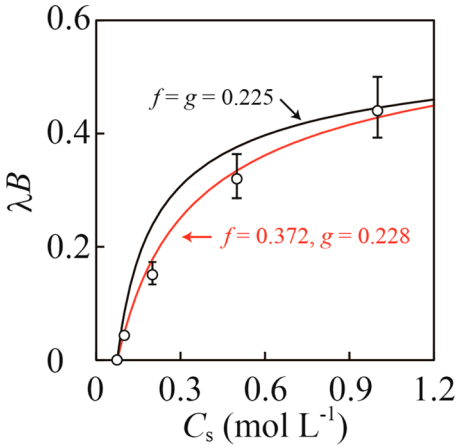

Figure 13. C_s dependence of the experimental values of λB for PMAPS in aqueous NaCl solutions, comprised with theoretical curves (solid lines) calculated from eq 26 using the indicated values of f and g.

experimental value of λB increases with the increasing C_s, implying that this phenomenon is typically called "anti-polyelectrolyte" solution behavior. According to Higgs and Joanny, the C_s dependence of an effective excluded-volume for the polyampholyte chains is a function of the sum of the nonrepulsive, the repulsive, and the attractive electrostatic interactions, which is predicted by the following equation:[8]

$$\lambda B = \lambda_0 B_0 + \frac{4\pi l_B (f-g)^2}{\kappa^2 a^3} - \frac{\pi l_B{}^2 (f+g)^2}{\kappa a^3} \quad (26)$$

where B_0 is the nonelectrostatic excluded-volume strength, a is the monomer size calculated by $a = d/2$, f is a fraction of positively charged monomer, and g is a fraction of negatively charged monomer. The value of d (1.68 nm) for PMAPS used the mean value estimated from R_H and $[\eta]$ in an aqueous NaCl solution, where the bead diameter taken as $d_B = 0.913d$.[51] For the experimental theta condition ($C_{s,\theta} = 0.074$ M for PMAPS), $\lambda B = 0$, the value of $\lambda_0 B_0$ was calculated from $\lambda_0 B_0 = -\beta_e + \beta_a$ to be 0.70. The comparison of the experimental C_s dependence of λB for PMAPS in an aqueous NaCl solution with theoretical curves (solid lines) calculated using eq 26 is shown in Figure 13. It can be seen that the experimental data are close to theoretical curve calculated by eq 26 using $f = 0.372$ and $g = 0.228$ or $f = 0.228$ and $g = 0.372$ rather than that for a neutral chains such as the sulfobetaine polymers ($f = g = 0.225$). The result implies that the net charge of PMAPS consisting of same number of positive and negative charged groups in an aqueous NaCl solution is not exactly zero. It is well-known that PMAPS in an aqueous NaCl solution at low salt concentration adsorb onto a silica particle[57] or silicon wafer,[58] of which surface is slightly negatively charged. Therefore, we suppose that net charge of PMAPS in an aqueous NaCl solution could be positive. The more sophisticated experimental salt-free approach is highly desirable because of determination of the precise sign of net charge for PMAPS.

4. CONCLUSIONS

The dilute solution properties of PMAPS with a wide range of M_w in aqueous NaCl solutions for C_s over a range from 0.074 M C_s to 1.0 M are thoroughly studied by LS, SAXS, and viscometry at 25 °C. The model parameters of M_L, λ^{-1}, d_H, d_B, δ, and B for PMAPS in aqueous NaCl solutions are successfully estimated from the M_w dependence of $\langle S^2 \rangle_z$, R_H, and $[\eta]$ based on the cylindrical wormlike chain model taking account the end effects. The M_w dependences of A_2 and Ψ for PMAPS are described in terms of the helical wormlike touched-bead model taking account the chain end effects using the obtained parameters. The C_s dependences of λ^{-1} and λB for PMAPS in an aqueous NaCl solution are in good agreement with the theoretical predictions calculated from eqs 25 and 26, respectively. From the parameters of f and g, the net charge of PMAPS in an aqueous NaCl solution is positive.

■ ASSOCIATED CONTENT

Supporting Information

The Supporting Information is available free of charge on the ACS Publications website at DOI: 10.1021/acs.macromol.5b01116.

Characterization results of the PMAPS samples in aqueous NaCl solutions at C_s = 0.074−1.0 M measured by SEC-MALS-Vis, DLS, and SAXS, the M_w dependence of ρ, plots of $A_2{}^{(E)}M_w$ versus $M_w{}^{-1}$, theories of A_2 and ψ (PDF)

■ AUTHOR INFORMATION

Corresponding Author

*E-mail takahara@cstf.kyushu-u.ac.jp; Ph +81-92-802-2517; Fax +81-92-802-2518 (A.T.).

Present Address

H.J.: Institute of Multidisciplinary Research for Advanced Materials, Tohoku University, 2-1-1, Katahira, Aoba-ku, Sendai 980-8577, Japan.

Notes

The authors declare no competing financial interest.

■ ACKNOWLEDGMENTS

The authors appreciate Professor Seigou Kawaguchi for helpful comments and suggestions which helped to improve this paper. The synchrotron radiation experiments were performed at beamline BL40B2 in the SPring-8 facility with the approval of the Japan Synchrotron Radiation Research Institute (JASRI) (Proposals Nos. 2009B1005 and 2010A1003).

■ REFERENCES

(1) Lowe, A. B.; McCormick, C. J. *Chem. Rev.* **2002**, *102*, 4177−4189.
(2) Dobrynin, A. V.; Colby, R. H.; Rubinstein, M. *J. Polym. Sci., Part B: Polym. Phys.* **2004**, *42*, 3513−3538.
(3) Kudaibergenov, S.; Jaeger, W.; Laschewsky, A. *Adv. Polym. Sci.* **2006**, *201*, 157−224.
(4) Tarannum, N.; Singh, M. *Rev. Adv. Sci. Eng.* **2013**, *2*, 90−111.
(5) Schlenoff, J. B. *Langmuir* **2014**, *30*, 9625−9636.
(6) Cranford, S. W.; Buehler, M. J. *Macromolecules* **2012**, *45*, 8067−8082.
(7) Ha, B.-Y.; Thirumalai, D. *J. Phys. II* **1997**, *7*, 887−902.
(8) Higgs, P. G.; Joanny, J.-F. *J. Chem. Phys.* **1991**, *94*, 1543−1554.
(9) Hirose, E.; Iwamoto, Y.; Norisuye, T. *Macromolecules* **1999**, *32*, 8629−8634.
(10) Schweins, R.; Hollmann, J.; Huber, K. *Polymer* **2003**, *44*, 7131−7141.
(11) Schulz, D. N.; Peiffer, D. G.; Agarwal, P. K.; Larabee, J.; Kaladas, J. J.; Soni, L.; Handwerker, B.; Garner, R. T. *Polymer* **1986**, *27*, 1734−1742.
(12) Huglin, M. B.; Radwan, M. A. *Polym. Int.* **1991**, *26*, 97−104.
(13) Mary, P.; Bendejacq, D. D.; Labeau, M.-P.; Dupuis, P. *J. Phys. Chem. B* **2007**, *111*, 7767−7777.
(14) Monroy Soto, V. M.; Galin, J. C. *Polymer* **1984**, *25*, 254−262.

DOI: 10.1021/acs.macromol.5b01116
Macromolecules 2015, 48, 7194−7204

(15) Huglin, M. B.; Radwan, M. A. *Makromol. Chem.* **1991**, *192*, 2433−2445.
(16) Kato, T.; Takahashi, A. *Ber. Bunsenges. Phys. Chem.* **1996**, *100*, 784−787.
(17) Terayama, Y.; Arita, H.; Ishikawa, T.; Kikuchi, M.; Mitamura, K.; Kobayashi, M.; Yamada, N. L.; Takahara, A. *J. Phys. Conf. Ser.* **2011**, *272*, 012010.
(18) Kikuchi, M.; Terayama, Y.; Ishikawa, T.; Hoshino, T.; Kobayashi, M.; Ogawa, H.; Masunaga, H.; Koike, J.; Horigome, M.; Ishihara, K.; Takahara, A. *Polym. J.* **2012**, *44*, 121−130.
(19) Kobayashi, M.; Terayama, Y.; Kikuchi, M.; Takahara, A. *Soft Matter* **2013**, *9*, 5138−5148.
(20) Liaw, D.-J.; Lee, W.-F.; Whung, Y.-C.; Lin, M.-C. *J. Appl. Polym. Sci.* **1987**, *34*, 999−1011.
(21) Duann, Y.-F.; Chen, Y.-C.; Shen, J.-T.; Lin, Y.-H. *Polymer* **2004**, *45*, 6839−6843.
(22) Jákli, G. Y. *J. Chem. Thermodyn.* **2007**, *39*, 1589−1600.
(23) Hai-Lang, Z.; Shi-Jun, H. *J. Chem. Eng. Data* **1996**, *41*, 516−520.
(24) Pike, E. R.; Pomeroy, W. R. M.; Vaughan, J. M. *J. Chem. Phys.* **1975**, *62*, 3188−3192.
(25) Terayama, Y.; Kikuchi, M.; Kobayashi, M.; Takahara, A. *Macromolecules* **2011**, *44*, 104−111.
(26) Kikuchi, M.; Lien, L. T. N.; Narumi, A.; Jinbo, Y.; Izumi, Y.; Nagai, K.; Kawaguchi, S. *Macromolecules* **2008**, *41*, 6564−6572.
(27) Berry, G. C. *J. Chem. Phys.* **1966**, *44*, 4550−4564.
(28) Provencher, S. W. *Comput. Phys. Commun.* **1982**, *27*, 213−227.
(29) Provencher, S. W. *Comput. Phys. Commun.* **1982**, *27*, 229−242.
(30) Ishikawa, T.; Kikuchi, M.; Kobayashi, M.; Ohta, N.; Takahara, A. *Macromolecules* **2013**, *46*, 4081−4088.
(31) Glatter, O.; Kratky, O. *Small Angle X-ray Scattering*; Academic Press: London, 1982.
(32) Benoit, H.; Doty, P. *J. Phys. Chem.* **1953**, *57*, 958−963.
(33) Hokajo, T.; Hanaoka, Y.; Nakamura, Y.; Norisuye, T. *Polym. J.* **2005**, *37*, 529−534.
(34) Amitani, K.; Terao, K.; Nakamura, Y.; Norisuye, T. *Polym. J.* **2005**, *37*, 324−331.
(35) Konishi, T.; Yoshizaki, T.; Saito, T.; Einaga, Y.; Yamakawa, H. *Macromolecules* **1990**, *23*, 290−297.
(36) Murakami, H.; Norisuye, T.; Fujita, H. *Macromolecules* **1980**, *13*, 345−352.
(37) Yamakawa, H.; Stockmayer, W. H. *J. Chem. Phys.* **1972**, *57*, 2843−2854.
(38) Yamakawa, H.; Shimada, J. *J. Chem. Phys.* **1985**, *83*, 2607−2611.
(39) Shimada, J.; Yamakawa, H. *J. Chem. Phys.* **1986**, *85*, 591−600.
(40) Domb, C.; Barrett, A. J. *Polymer* **1976**, *17*, 179−184.
(41) Einaga, Y.; Abe, F.; Yamakawa, H. *Macromolecules* **1993**, *26*, 6243−6250.
(42) Yamakawa, H. *Macromolecules* **1992**, *25*, 1912−1916.
(43) Yamakawa, H.; Fujii, M. *Macromolecules* **1973**, *6*, 407−415.
(44) Norisuye, T.; Motowoka, M.; Fujita, H. *Macromolecules* **1979**, *12*, 320−323.
(45) Barrett, A. J. *Macromolecules* **1984**, *17*, 1561−1565.
(46) Yoshizaki, T.; Nitta, I.; Yamakawa, H. *Macromolecules* **1988**, *21*, 165−171.
(47) Kirkwood, J. G.; Riseman, J. *J. Chem. Phys.* **1948**, *16*, 565−573.
(48) Barrett, A. J. *Macromolecules* **1984**, *17*, 1566−1572.
(49) Norisuye, T.; Fujita, H. *Polym. J.* **1982**, *14*, 143−147.
(50) Yoshizaki, T.; Yamakawa, H. *Macromolecules* **1980**, *13*, 1518−1525.
(51) Nagasaka, K.; Yoshizaki, T.; Shimada, J.; Yamakawa, H. *Macromolecules* **1991**, *24*, 924−931.
(52) Odijk, T. *J. Polym. Sci., Polym. Phys. Ed.* **1977**, *15*, 477−483.
(53) Skolnick, J.; Fixman, M. *Macromolecules* **1977**, *10*, 944−948.
(54) Tamai, Y.; Konishi, T.; Einaga, Y.; Fujii, M.; Yamakawa, H. *Macromolecules* **1990**, *23*, 4067−4075.
(55) Fujii, Y.; Tamai, Y.; Konishi, T.; Yamakawa, H. *Macromolecules* **1991**, *24*, 1608−1614.
(56) Dehara, K.; Yoshizaki, T.; Yamakawa, H. *Macromolecules* **1993**, *26*, 5137−5142.
(57) Starck, P.; Mosse, W. K. J.; Nicholas, N. J.; Spiniello, M.; Tyrrell, J.; Nelson, A.; Qiao, G. G.; Ducker, W. A. *Langmuir* **2007**, *23*, 7587−7593.
(58) Kato, T.; Kawaguchi, M.; Takahashi, A. *Langmuir* **1999**, *15*, 4302−4305.

DOI: 10.1021/acs.macromol.5b01116
Macromolecules 2015, 48, 7194−7204